Available online at www.sciencedirect.com
ScienceDirect
Ceramics International 37 (2011) 2737–2746
CERAMICS INTERNATIONAL
www.elsevier.com/locate/ceramint

Structural discrepancies and in vitro nanoapatite formation ability of sol–gel derived glasses doped with different bone stimulator ions

Sara Shahrabi, Saeed Hesaraki *, Saeed Moemeni, Mina Khorami

Nanotechnology and Advanced Materials Department, Materials and Energy Research Center, Karaj, P.O. Box 31787/316, Iran

Received 15 January 2011; received in revised form 12 April 2011; accepted 14 April 2011
Available online 21 April 2011

Abstract

In this study, sol–gel derived glasses were prepared based on the following general formula: $25CaO–5MO–70SiO_2$ (M = Ca, Sr, Zn), and development of a calcium phosphate (CP) layer on their surfaces was studied by soaking them in a simulated body fluid (SBF) for different periods. The consequent formation of the CP layer and structural discrepancies of the formed layer of various glasses were studied by means of appropriate techniques such as X-ray diffractometry, Fourier transform infrared spectroscopy and scanning electron microscopy equipped with an energy dispersive system (EDS). The concentration of Ca, Si and M ions released from the samples into the SBF was measured by using inductively coupled plasma-atomic emission spectroscopy. The effect of compositional changes on proliferation and activity of osteoblastic cells was evaluated by employing rat calvaria-derived cells.

According to the mechanism reported in the literature a SiO_2-rich layer was initially formed on the surfaces of all glasses exposed to SBF. The results showed that CP formation ability of the glasses was strongly dependent on its chemical compositions. It was observed that the ability of calcium phosphate formation on the glass surfaces was inhibited by ZnO substitution, whereas the ternary $CaO–SrO–SiO_2$ system exhibits progressively improved nanostructured carbonated apatite layer on the glass surfaces in comparison to binary $CaO–SiO_2$ glass. The results of cell culture tests revealed that both Zn and Sr had stimulatory effect on cell responses; the rate of cell proliferation was enhanced by the former and alkaline phosphatase activity was improved by the latter.

Keywords: Bioglass; Strontium; Zinc; Bone filler; Nanoapatite

1. Introduction

Bioactive glasses and glass-ceramics have been extensively investigated for important applications in medicine to repair or replace bones [1]. These materials can bind to a living bone through the formation of an apatite like layer on their surfaces [2]. Bioglasses can be synthesized by melting and sol–gel methods, but the latter is preferred because of higher compositional range of bioactivity and higher surface area that results in better binding to the living tissues [3].

Since the discovery of the first bioglass by Hench et al. several other glass compositions have been imposed to improve the rehabilitation process in surgical applications. One of the important trends in recent studies is incorporation of some ions in the bioglass composition to improve its biofunctionallity. Regarding the stimulatory effects of some cations such as Mg^{2+}, Sr^{2+} and Zn^{2+} on bone formation either by oral administration or local delivering process [4], the effect of incorporation of these ions on the physical and physicochemical properties of sol–gel derived glasses has been reported. However, due to the strong dependence of glass bioactivity to its chemical composition, there are contradictory reports for the effect of incorporation of these ions on the surface reactivity of bioglasses, because of the compositional variety of the studied systems. For example, Oki et al. [5] synthesized $SiO_2–CaO–ZnO–P_2O_5$ bioglass through the sol–gel method and revealed that the synthesized glass has the ability of apatite formation after confronting with simulated body fluid (SBF) solution. In contrary, Aina et al. [6] reported the inhibited bioactivity of zinc-doped melt-derived $SiO_2–P_2O_5–CaO–Na_2O$ based glass. While Hesaraki et al. [7] showed that the rate of apatite formation of a $CaO–SiO_2–P_2O_5$ bioglass was reduced by

* Corresponding author. Tel.: +98 2616204131 4; fax: +98 2616201888.
E-mail address: S-hesaraki@merc.ac.ir (S. Hesaraki).

0272-8842/$36.00
doi:10.1016/j.ceramint.2011.04.025

substitution of SrO for CaO (up to 10 mol.%), Lao et al. [8] stated that Sr substitution enhanced bioactivity of $CaO–SiO_2$ based glass.

Due to the diversity of the studied bioglass systems and difference in concentrations of the substituted ions, comparative statement on the effect of these ions on glass bioactivity is also inexplicable. In other words, it is difficult to state that Zn improves glass bioactivity or strontium retards glass surface reactivity in general, because the studies have not been performed on the same glass composition using the same substituting concentrations.

In this study, a simple binary bioactive glass, i.e. $CaO–SiO_2$was selected and synthesized by sol–gel method. 5 mol. % of CaO was substituted by the same amount of zinc and strontium ions and the effect of these substitutions on the apatite formation ability of the bioglasses and the structural properties of the formed layer was studied.

2. Materials and method

2.1. Formulation and synthesis of glasses

Bioactive glasses were formulated based on $25CaO–5MO–70SiO_2$system in which M was Ca, Zn, and Sr. Table 1 shows the nominal composition of the synthesized glasses. Sol–gel method according to Oki et al. [5] was employed for the synthesis of the glasses. In brief tetraethoxyorthosilicate (TEOS) hydrolysis was carried out using 1 M HNO_3 as catalyst. The solutions were stirred for 45 min after the addition of each reactant (TEOS, calcium nitrate and zinc/strontium nitrate) for 1 h more after the last addition. The prepared sols were separately poured in sealed cylindrical Teflon containers and kept at room temperature for 3 days to allow gel formation. The gels were then aged at 70 °C for 72 h and dried at 120 °C for 48 h.

To estimate firing temperature for stabilizing glass composition (for removal of residual organic and nitrate precursors without any crystallization state), simultaneous thermal analysis (STA) measurement was carried out on dried, powdered bioactive glass samples up to 1200 °C, at heating rate of 5 °C/min, using a powdered alumina as reference material.

To achieve stabilized compositions, dried gels were heated at 700 °C for 4 h in an electric furnace.

2.2. In vitro bioactivity assessment

The glass powder (the fired gel) was ground in agate mortar to an average particle size of 10 μm, weighed and shaped to discs (10 mm in diameter and 3 mm in thickness) with a hydraulic press under 9 MPa pressure. The discs were re-heated at 700 °C for 3 h to improve its mechanical stability. These samples with the same shape surface area were used in both in vitro and cell behavior assessments. The in vitro assays were carried out by soaking each glass specimen in polyethylene bottles containing 25 ml of simulated body fluid and maintained at 37 °C for different intervals. The medium of each container was renewed at defined interval times up to 500 h. The SBF solution with inorganic chemical composition resembling that of blood plasma was prepared according to the Kokubo's specification [9].

Table 1
Nominal composition (mol.%) of the synthesized glasses.

Sample	SiO_2	CaO	SrO	ZnO
BG-Ca	70	30	0	0
BG-Sr	70	25	5	0
BG-Zn	70	25	0	5

Change in concentration of Ca^{2+}, Si^{4+} and M^{2+} ions of the SBF was measured by inductively coupled plasma-atomic emission spectroscopy technique. It should be noted that the concentration of the above mentioned ions in fresh SBF solution has been excluded from the obtained results when reporting data.

Changes in phase composition of the specimens were determined by X-ray diffractometry (XRD). For this purpose, after each interval, the samples were withdrawn from the solution and washed with distilled water gently, dried at room temperature, ground to fine powder and their X-ray diffraction patterns were collected using a Philips PW3710 X-ray diffractometer with Ni filter and Cu target. Data were identified by ASTM standard diffraction Cards. The patterns of unsoaked bioactive glass specimens were also taken for comparison.

FTIR spectra of the bioactive glasses were measured at room temperature in the wave number range of 4000–400 cm^{-1} using a Fourier transform infrared spectrometer (Vector Bruker 33). Fine powders were mixed with KBr powder by the ratio of 1:100 and transparent homogenous discs were formed by pressing the mixture under 5 ton/cm^2 pressure. The FTIR spectra were immediately measured after preparation of the disc.

The surface morphologies of the specimens were observed by scanning electron microscope (SEM) operated at accelerating voltage of 20 kV and current intensity of 10 mA. Because of the poor electrical conductivity of the samples, their surfaces were coated with a thin layer of gold before the test. Elemental image analysis was also carried out using energy dispersive X-ray analysis (EDXA) coupled to the SEM instrument.

2.3. Cell behavior studies

Osteoblastic cells were extracted from the rat calvarium as mentioned elsewhere [10] and cultured in a medium consisted of Dulbecco modified Eagle medium (DMEM; Gibco-BRL, Life Technologies, Grand Island, NY) supplemented with 15% fetal bovine serum (FBS; Dainippon Pharmaceutical, Osaka, Japan) and 100 g/mL penicillin–streptomycin (Gibco-BRL, Life Technologies). The cell suspensions were cultured in polystyrene 6-well dishes. Nonadherent cells were removed from the cultures after 4 days by a series of phosphate buffered saline (PBS) washes and subsequent medium changes. Adherent cells were expanded as monolayer cultures in a 5% CO_2/95% air atmosphere at 37 °C with medium changes

every 3 days. The confluent cells were dissociated with trypsin and subcultured in new 6-well culture dishes at a plating density of 6×10^4 cells/dish. These handlings were repeated several times until sufficient number of cells was produced.

The disc-shaped bioglass specimens (6 mm in diameter and 3 mm in height) were sterilized using 70% ethanol and the cells were seeded on tops of the glass discs at 1×10^4 cells/disc. The specimen/cell constructs were placed into 24-wells culture plates and left undisturbed in an incubator for 3 h to allow the cells to attach to them and then an additional 3 ml of culture medium was added into each well. The cell/specimen constructs were cultured in a humidified incubator at 37 °C with 95% air and 5% CO_2 for 1, 7 and 14 days. Note that, every 3 days, the medium was exchanged.

The proliferation of the osteoblastic cells on bioglass specimens was determined using the MTT (3-{4,5-dimethylthiazol-2yl}-2,5-diphenyl-2H-tetrazolium bromide) assay. For this purpose, at the end of each evaluating period, the medium was removed and 2 ml of MTT solution was added to each well. Following incubation at 37 °C for 4 h in a fully humidified atmosphere at 5% CO_2 in air, MTT was taken up by active cells and reduced in the mitochondria to insoluble purple formazan granules. Subsequently, the medium was discarded and the precipitated formazan was dissolved in dimethylsulfoxide, DMSO (150 ml/well), and optical density of the solution was read using a microplate spectrophotometer (BIO-TEK Elx 800, Highland park, USA) at a wavelength of 570 nm.

To observe the morphologies of the cells attached onto the surfaces of the glass specimens, the cells were cultured onto the glass discs as described above. After 14 days, the culture medium was removed, the cell-cultured specimens were rinsed with phosphate buffered saline (PBS) twice and then the cells were fixed with 500 mL/well of 3% glutaraldehyde solution (diluted from 50% glutaraldehyde solution (Electron Microscopy Science, USA) with PBS). After 30 min, they were rinsed again and kept in PBS at 4 °C. Specimens were then fixed with 1% Osmium tetroxide (Polyscience, Warmington, PA, USA). After cell fixation, the specimens were dehydrated in ethanol solutions of varying concentration (30, 50, 70, 90, and 100%) for about 20 min at each concentration. The specimens were then dried in air, coated with gold and analyzed by SEM (Streoscan S 360, Cambridge).

The osteoblast activity was determined by measuring the level of alkaline phosphatase (ALP) enzyme. The cells were seeded on the samples under the same culturing condition described elsewhere and the level of ALP was determined on days 1, 7 and 14. The osteoblasts lysates were frozen and thawed three times to disrupt the cell membranes. ALP activity was determined at 405 nm using p-nitrophenyl phosphate in diethanolamide buffer as chromogenic substrate.

In FTIR spectroscopy, cell proliferation and ALP tests, four sample of each composition were tested and each experiment was repeated three times. Data were processed by Microsoft Excel (2003) and the results were presented as mean ± standard deviation. Significance between the mean values was calculated using standard software program (SPSS GmbH, Munich, Germany) and the $p \leq 0.05$ was considered significant.

3. Results

3.1. Thermal analysis

Fig. 1 shows the differential thermal analysis (DTA) curves of various gels after drying at 120 °C. A DTA trace is a plot of heat changes of the glass as a function of temperature and is used to determine temperatures at which phase transitions or another thermal phenomenon occur.

In all samples, the first endothermic peak which initiated at room temperature corresponds to the release of physically adsorbed water and the pore liquor (water and by-products from the polycondensation reaction) that were not removed during drying.

The second endothermic peak (onset at 433 °C) was due to the condensation of silanol groups and the removal of nitrate groups that are usually eliminated in the thermal stabilization process. All nitrates were removed by 550 °C. However, the significant effect of Sr and Zn cations substituted for Ca in the bioglass composition is the changes in glass transition (Tg) and crystallization (Tc) temperatures. From the DTA traces, the glass transition temperature is 760 °C for BG-Ca, 750 °C for BG-Sr and 716 °C for BG-Zn. Also, the large exothermic peak corresponded to crystallization of the glasses is appeared at 951 °C for BG-Ca, 959 for BG-Sr and 921 °C for BG-Zn. According to the results of DTA, all glasses were stabilized at 700 °C, because nitrates are completely eliminated from the glass composition and no crystallization phenomenon occurs.

3.2. Ion chemistry of SBF

Fig. 2 shows the changes in Ca, Si and M (Sr and Zn) concentration of the SBF solution of various glasses during the soaking procedure. Since apatite precipitation on the glass surfaces occurs through a dissolution–precipitation process which has been discussed in literatures [11] and concerning this

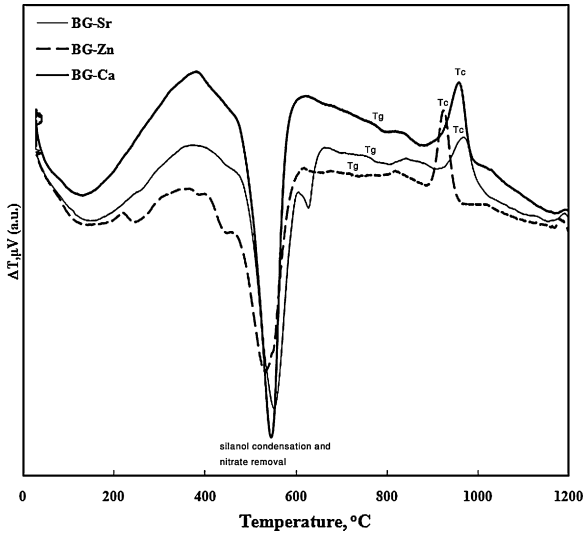

Fig. 1. The differential thermal analysis (DTA) curves of various gels after drying at 120 °C (Tg: glass transition temperature, Tc: crystallization temperature).

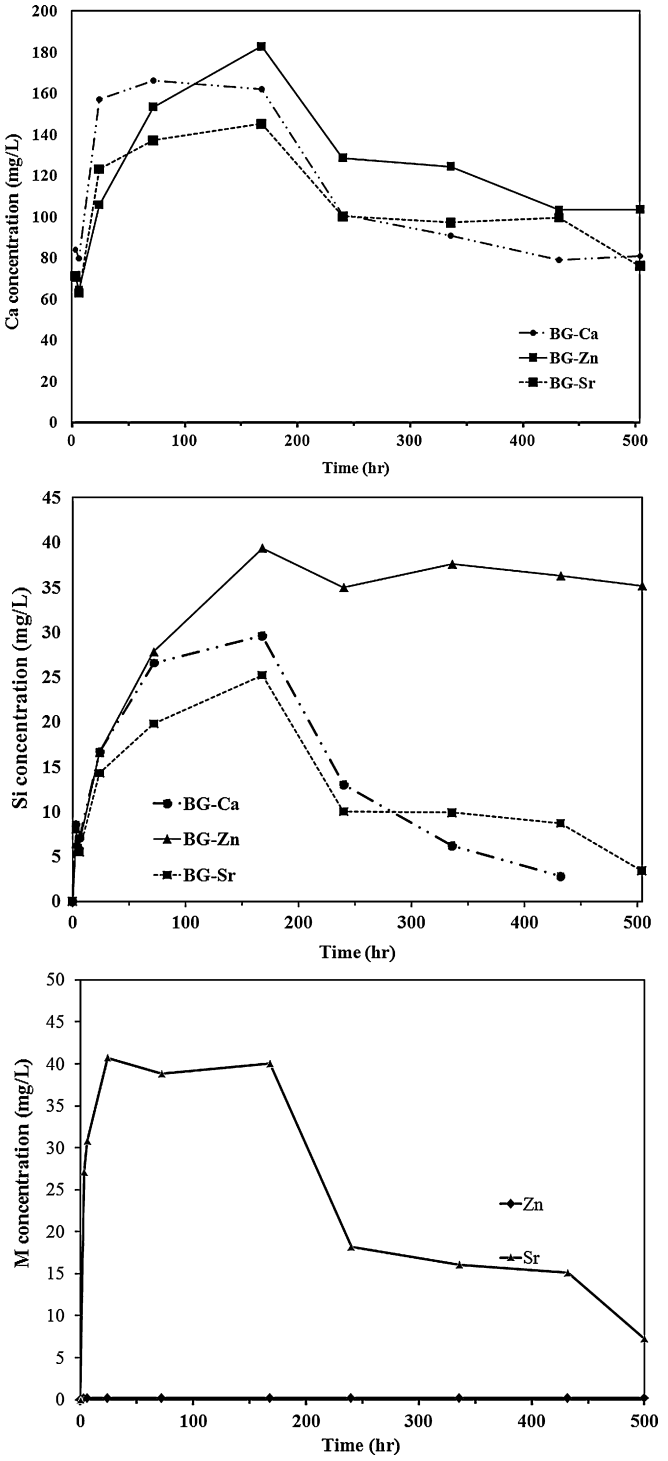

Fig. 2. The changes in Ca, Si and M (Sr and Zn) concentration of the SBF solution of various glasses during the soaking procedure.

fact that the concentration of the above mentioned ions in fresh SBF solution has been excluded from the experimental data, appearance of positive values for Ca^{2+} concentration in the graphs means that dissolution phenomenon always overcomes to precipitation. For BG-Sr and BG-Ca, a rapid increase in the Ca^{2+} concentration occurs during the early stages of the immersion ranging from 3 h to 24 h, followed by slight change up to 168 h and a decrease after that. It can be stated that the rate of dissolution decreases after 168 h due to active precipitation process. For Ca-Zn, the Ca concentration increases during 168 h of evaluation and then decreases up to 500 h. It can be observed that, after 168 h (7 days), the Ca^{2+} concentration of SBF solutions of BG-Sr and BG-Ca is lower than that of BG-Zn. On the one hand, zinc cation that was replaced for Ca in gel-derived $CaO–SiO_2$ system, diminished the calcium contribution for the apatite crystallization while strontium revealed a promising role in Ca consumption for calcium phosphate precipitation. Fig. 2 reveals that lower amounts of Si ions are found in the SBF solutions of BG-Sr and BG-Ca compared to BG-Zn. Difference in Si concentrations is cleared after 72 h. The Si concentration of the BG-Sr and BG-Ca solutions sharply decreases after 168 h whereas it remains constant in the case of BG-Zn. The decreased Si concentration of SBF solution can be assigned to its contribution in formation of Si–O–Si layer on the glass surface, its consumption for the formation of silicate doped apatite phase and/or its limited release due to the formed apatite layer.

The Sr and Zn ion concentrations in the SBF solution have been also compared in Fig. 2. The BG-Sr glass releases Sr ions from its composition into the SBF during 24 h. The rate of release is constant from 24 h to 168 h and then sharply decreases. It is suggested that the released Sr ions migrate into the lattice of apatite to form a Sr-doped phase. There are also other suggestions: (i) The release of Sr ions from the glass structure is restricted by the formed apatite layer, (ii) Sr ions are not released from the Sr-doped apatite layer which is a chemically stable compound. For all periods of evaluation, the concentration of Zn ions in the SBF solution is always lower than 0.2 ppm. These results show that the Zn ions have not been easily delivered from the BG-Zn glass.

3.3. Structural groups

FTIR is sensitive to the materials local structure and it is quite useful to distinguish the materials structural changes. For silicate glasses, the analysis of FTIR is usually accomplished by determining the changes of vibrational modes in frequency and intensity.

Fig. 3 shows the FTIR spectra of all synthesized glasses before and after soaking in SBF solution for different periods (up to 14 days). All bands are marked with their corresponding vibrational/stretching mode of structural groups. For unsoaked glasses, the bands appeared in the range 800–1100 cm^{-1} are ascribed to the stretching modes of SiO_4 tetrahedra. The wide absorption band at 1000–1100 $cm^{-1}$is assigned to the asymmetric stretching mode Si–O (asym), the one weak band around 800 cm^{-1} is associated to symmetric stretching vibration Si–O–Si (sym) and the Si–O group with one non-bridging oxygen (NBO) atom is found at 950 cm^{-1}. Furthermore, the band at 470 cm^{-1} can be ascribed to the Si–O–Si bending mode. The signal at around 1630 cm^{-1} is also assigned to deformation mode of H–O–H group attributed to the absorbed water molecules.

In the case of Sr-BG and Ca-BG glasses soaked in SBF for 7 and 14 days, a progressive evolution in SiO_4 IR spectra can be

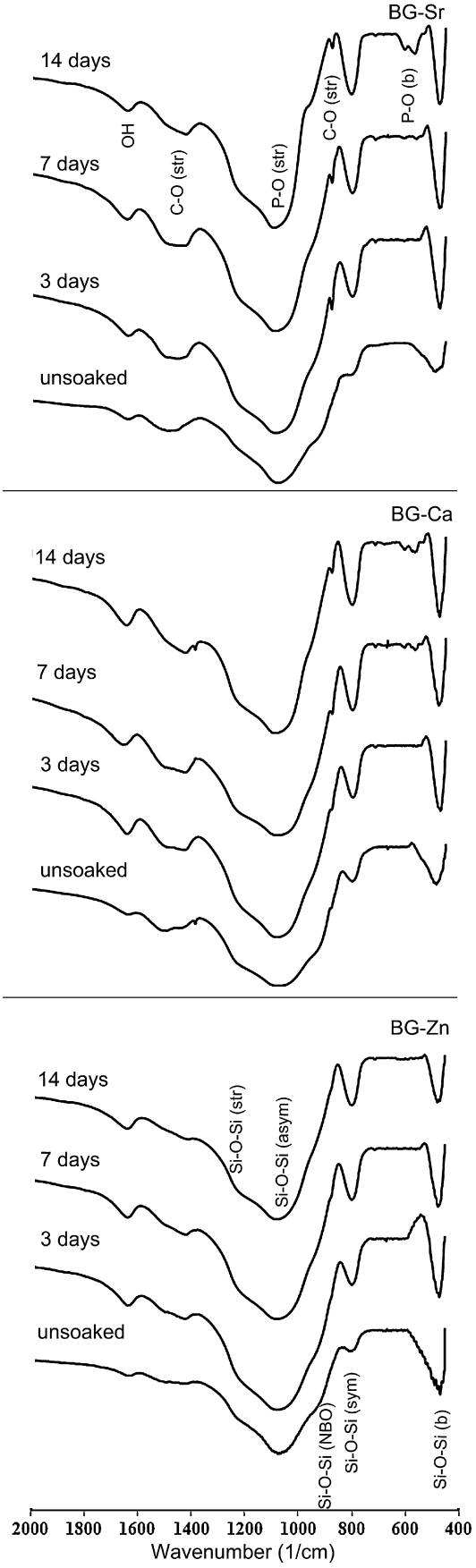

Fig. 3. The FTIR spectra of various synthesized glasses before and after different soaking periods.

seen, meanwhile new bands are also appeared at around 570, 600 and 870 cm^{-1}. The sharpened bands in the range of 800–1100 cm^{-1} are probably due to the formation of silica gel like layer on the surfaces of these glasses [12]. The peaks at 570 and 600 cm^{-1} are associated with the P–O bending mode of crystalline phosphate (apatite) formed on the glasses and the shoulder appeared at 870 cm^{-1} is attributed to the stretching (str) mode of C–O group in the lattice structure of the formed apatite layer. The absorption band at around 1050 cm^{-1} associated with the P–O stretching has an overlap with Si–O–Si (asy) and thus is not clearly distinguishable. From the FTIR data, it can be stated that the phosphate layer is formed on BG-Ca and BG-Sr glasses after soaking in SBF solution for 7 days. After 14 days soaking, the intensity of P–O bands in FTIR spectrum of the soaked BG-Sr glass is much higher than that of BG-Ca, indicating progressively grown apatite crystals on its surfaces which is in agreement with XRD data. In contrary, no considerable changes are observed in FTIR spectra of BG-Zn glass before and after soaking in SBF, except little sharpening in SiO_4 bands after the soaking process. No signs of phosphate formation are also observed for this glass. These results reveal accelerating effect of SrO and inhibiting role of ZnO on bioactivity of $70SiO_2$–30CaO glass.

3.4. Phase composition

The XRD patterns of all glasses before and after different soaking intervals are shown in Figs. 4–6. It is revealed that all samples show the characteristic of amorphous material before the soaking procedure, because no peaks are detected in their XRD patterns. Soaking for one day also makes no changes in diffraction patterns of all samples. After 3 days of immersion, the patterns of BG-Sr (Fig. 4) shows the existence of a broad

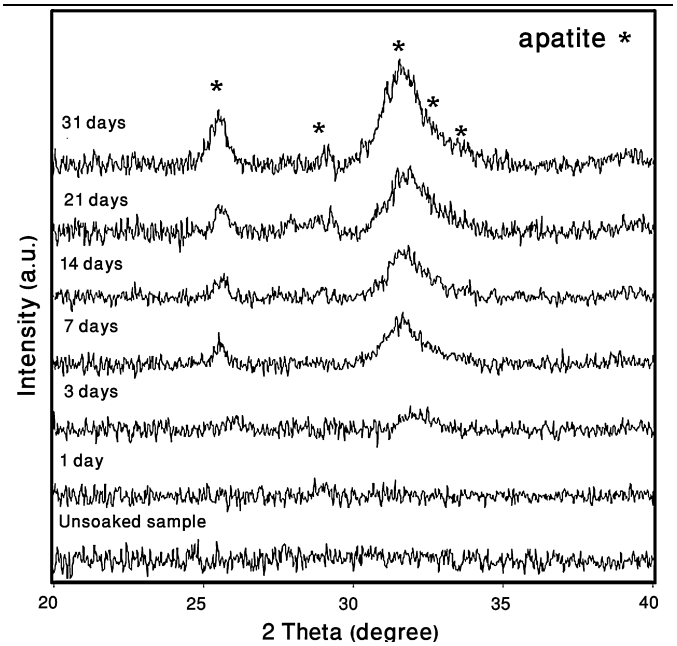

Fig. 4. The XRD patterns of BG-Sr glass before and after different soaking intervals.

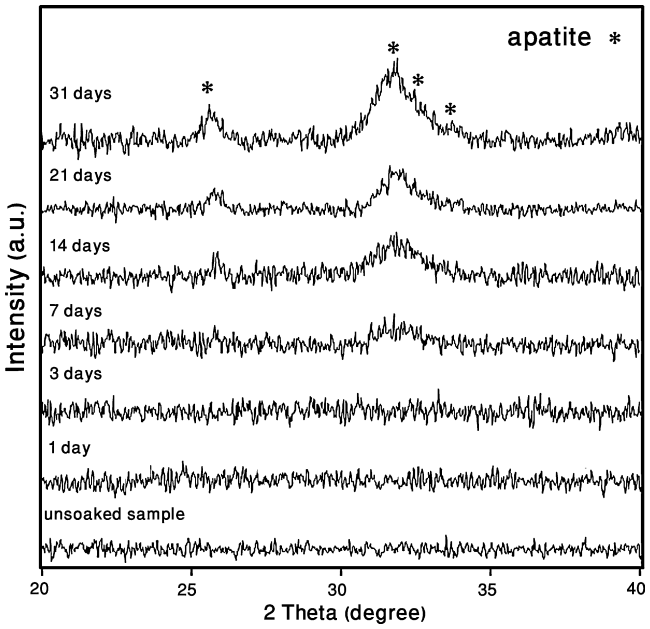

Fig. 5. The XRD patterns of BG-Ca glass before and after different soaking intervals.

peaks at $2\theta = 31.8^\circ$ which is characteristic of (2 1 1) atomic plane diffraction of apatite phase (JCPD 24-003). In BG-Ca (Fig. 5), the (2 1 1) diffraction pattern is appeared after 7 days of immersion. The diffraction pattern corresponding to (0 0 2) atomic plane of apatite phase ($2\theta = 25.9^\circ$) is clearly observed after 7 days for BG-Sr and after 14 days for BG-Ca. In both samples (BG-Sr and BG-Ca), the intensity of apatite peaks increase with increasing soaking time up to 31 days, meanwhile the appearance of new peaks at $2\theta = 32.18^\circ$, 32.86° (attributed to the crystallization of (1 1 2) and (3 0 0) atomic planes in apatite lattice), $2\theta = 28.9^\circ$ and 39.7° (assigned to the crystallization of (2 1 0) and (1 3 0) atomic planes in apatite lattice) demonstrate the maturity of the formed apatite layer on the glass surfaces. At the same time intervals, the diffraction intensities of all atomic planes of apatite phase formed on Sr-doped glass are higher than that formed on $CaO–SiO_2$ system. These results can approve the accelerating effect of Sr ions on apatite formation ability of $SiO_2–CaO$ based bioglass which is in agreement with previous studies reported for other systems [13]. The XRD pattern of BG-Zn specimen (Fig. 6) is totally different with others. No changes were observed in the pattern of this specimen even after soaking in SBF for 31 days. It reveals that the Zn ion inhibits the formation of apatite layer on the glass surface strongly. BG-Sr specimen shows the most bioactivity among the glasses whereas Zn-containing sample fails to form an apatite layer in vitro.

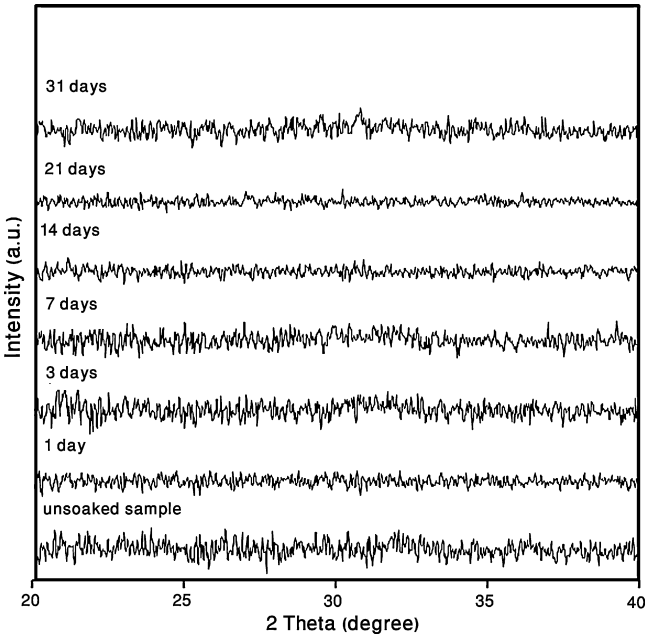

Fig. 6. The XRD patterns of BG-Zn glass before and after different soaking intervals.

3.5. Surface morphology and elemental composition

Fig. 7 shows the SEM micrographs of various glasses soaked in SBF solution for 14 and 31 days. The EDS patterns of 31-days soaked samples related to the above SEM images are also shown in Fig. 8. Microstructure of the soaked BG-Sr comprises of well grown flake-like crystals with tight entanglement whereas in BG-Ca ball like particles that composed of too many wrinkled type crystals are observed. The microstructure of BG-Zn is totally different to that of other samples and polygonal particles with smooth surface are observed after 14 days which tend to a relatively rough surface after 31 days. No signs of precipitation are observed in BG-Zn micrograph even after 31 days of soaking. The elemental image analyses of BG-Sr and BG-Ca specimens carried out by EDS show the presence of P and Ca as the main elements of each glass surface and confirm that the formed layers are calcium phosphatic in nature. No peaks corresponding to impurities are observed. The presence of Si peak with reduced intensity is also noticeable. It originates from the underneath layer (glass) and its reduced peak intensity reveals considerable thickness of the formed layer.

In BG-Zn specimen, although phosphorous is also found in its elemental composition, concentration of Si is considerable. The results suggest that a thin layer of calcium phosphate may be formed on Zn-containing glass which cannot be detected by XRD technique because of its low concentration with respect to the bulk volume. The appearance of Si element in EDS pattern of this specimen indicates the extenuation of the formed calcium phosphate layer. The peak corresponded to Cl suggests that this ion is incorporated into the crystal structure of apatite or adsorbed on glass surfaces from the SBF despite of washing process.

3.6. Cell proliferation, activity and morphology

The proliferation and ALP of the osteoblastic cells cultured on various specimens for different times are shown in Fig. 9(a) and (b), respectively. After cell attachment, the osteoblasts began a period of proliferation on all specimens confirmed by the difference in the cell number between days 1, 7 and 14

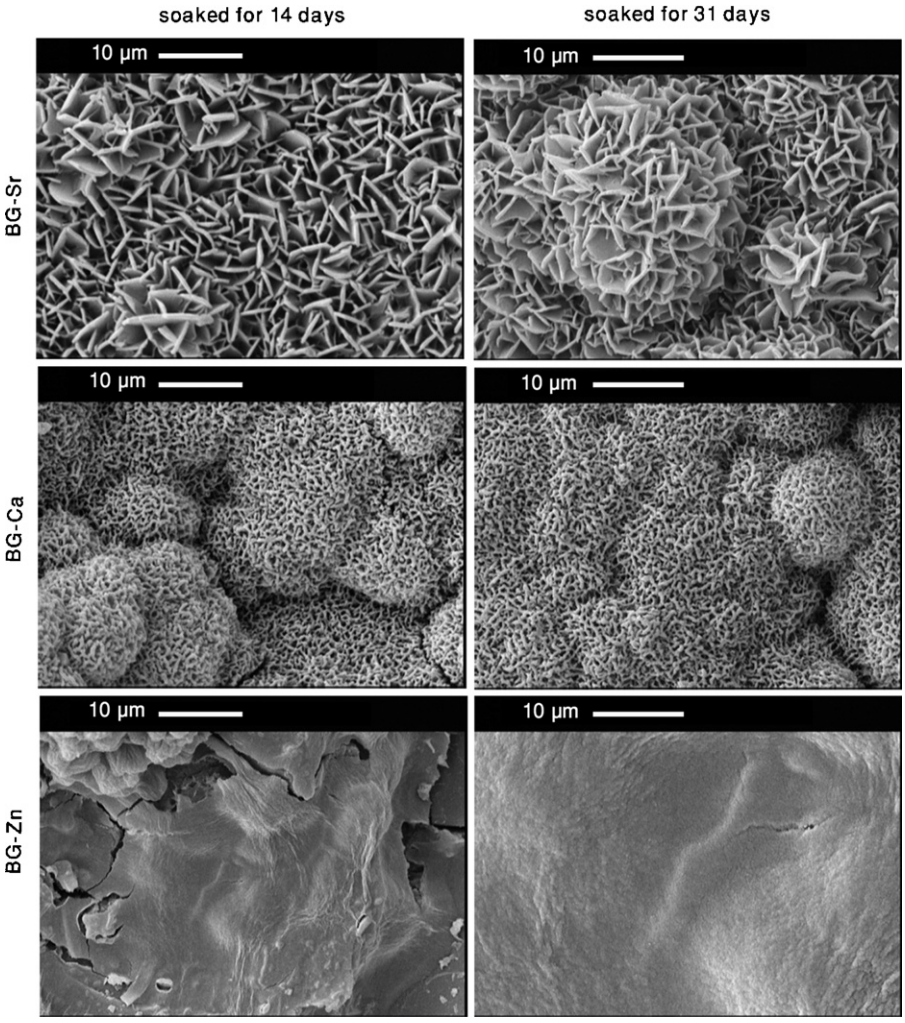

Fig. 7. The SEM micrographs of various glasses soaked in SBF solution for 14 and 31 days.

($p < 0.05$). At 1st day, no significant difference is observed between the cell numbers of BG-Ca, BG-Sr and BG-Zn ($p \gg 0.05$). At both 7th and 14th days, the amount of formazon produced by osteoblasts cultured on BG-Zn glasses is significantly higher than that of two other glasses, meanwhile the difference between the number of cells proliferated on BG-Ca and BG-Sr is not statistically significant.

Alkaline phosphatase is known as an early osteoblastic differentiation marker [14] and is produced by the cells showing mineralized extracellular matrix. Fig. 9(b) shows normalized ALP activity of osteoblastic cells on glasses. For all specimens, ALP activity increases from 1st day to 7th day of culture ($p < 0.05$) and then is inhibited on 14th day ($p < 0.05$) probably due to conflux of the expanded cells. At day 7th, higher level of ALP is observed for BG-Sr compared to BG-Ca and BG-Zn glasses ($p < 0.05$). The difference between ALP activity of BG-Ca and BG-Zn is also significant ($p > 0.05$). These data actually suggest that the cells on BG-Sr differentiated more than that on BG-Ca and BG-Zn. Since cells that differentiate generally do not proliferate quite, the number of cell on BG-Sr is lower than that of BG-Zn.

The above mentioned suggestion is confirmed by the SEM image of the cells cultured on the glasses (Fig. 10). Confluent cells with extended sytoplasmic membrane have been spread on glasses with different surface morphologies. In BG-Sr and BG-Ca, the cells have entangled themselves to needlelike nanosized crystals produced in cell culture medium due to their bioactive nature. In BG-Zn however, more extended cells are observed on glass surface which confirms the MTT results. The surface morphology of all glasses soaked in cell culture medium is also in agreement with those soaked in SBF solution.

4. Discussion

The purpose of this investigation was to study the influence of Sr^{2+} and Zn^{2+} substitutions for Ca^{2+} (5 mol.%) on the apatite formation ability of $CaO–SiO_2$ based bioactive glass. It has been reported that these cations enhance bone healing process when using in bioglass compositions despite their different roles in the glass structure. Oxides such as SiO_2 and P_2O_5 act as network formers in the glass structure which are responsible for producing bridging oxygen (BO) atoms. It has been believed

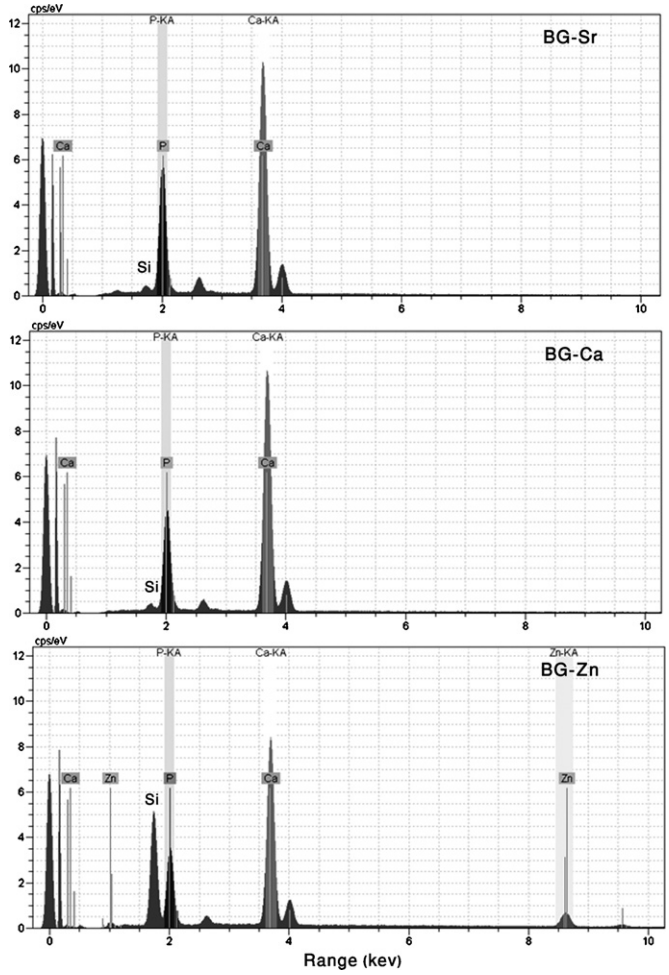

Fig. 8. The EDS patterns of 31-days soaked samples related to SEM images.

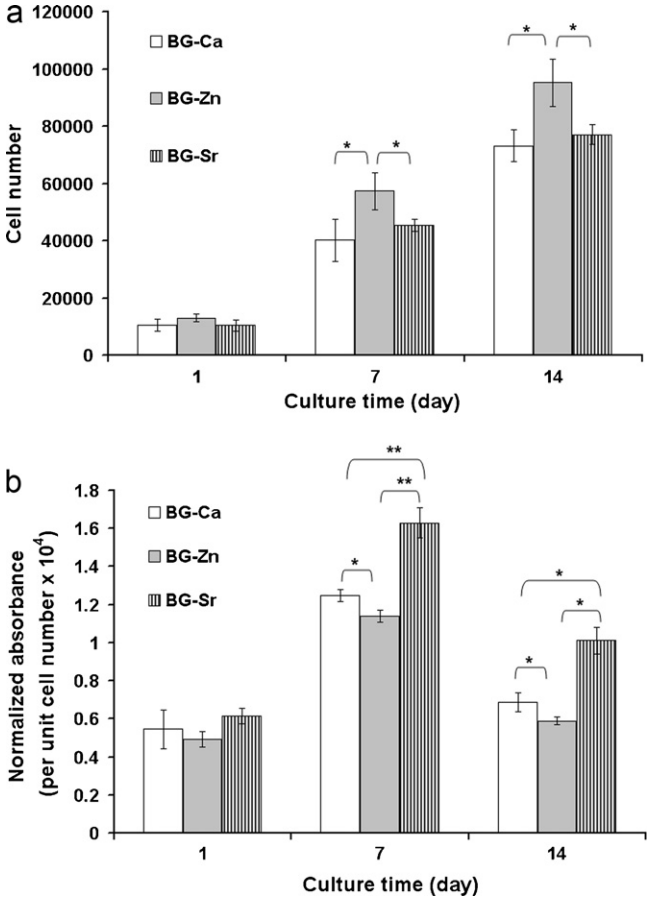

Fig. 9. Proliferation (a) and normalized alkaline phosphatase activity (b) of osteoblasts cultured on various glasses as a function of time (*$p < 0.05$, **$p < 0.01$).

that CaO has a network modifying role in the glass structure that produces non-bridging oxygen (NBO) atoms. To determine the degree of glass bioactivity using such substitutions, it is critical to have a structural understanding of each substituted cations within the glass.

Since SrO and ZnO are replaced for CaO, they are expected to act as network modifier. Authors showed the role of each substituted ions in the glass structure using some experiments including FTIR and DTA. For example, Chen et al. [15] revealed that the peak intensity ratio of NBO to BO (i.e. the Si–O–NBG/Si–O–Si) in FTIR spectra reduced by substitution of MgO for CaO in SiO_2–CaO–P_2O_5 ternary system. Watts et al. [16] showed that magnesium acts more as an intermediate oxide than modifier when replaced for CaO in SiO_2–CaO–P_2O_5 glass. Decrease in Tg and Ts (softening temperature) and increase in thermal expansion coefficient of MgO substituted glasses was mentioned as a supporting data for their hypothesis due to the weakened glass structure. They suggested that the substituted Mg forms MgO_4^{2-} species in the glass structure with Si–O–Mg bonds that exhibit lower bond strength than Si–O–Si results in reduced Tg and Ts. The same results were obtained by Linati et al. [17] who investigated ZnO substituted glasses.

In this study, the bands appeared at 800 and 1100 cm^{-1} of the FTIR spectra of glasses (Fig. 3), are assigned to Si–O–Si groups that produce BO and the band arises at 950 cm^{-1} relates to Si–O– (NBO). Table 2 estimates the relative ratio between IR absorbance for Si–O groups with BO and NBO as well as glass transition temperature as a function of substituted cations. There is no significant difference between the intensity ratios of Si–O–BO/Si–O–NBO for BG-Ca and BG-Sr glasses whereas it significantly ($p < 0.05$ for at least five measurements) increases by substituting Zn for Ca. It means that the average number of bridging oxygen in BG-Zn is higher than that of BG-Sr and BG-Ca.

As observed in Table 2, substitution of Sr for Ca in the glass composition caused slight decrease in Tg (∼10 °C), while Tg was considerably diminished by Zn replacement (∼44 °C). These results suggest that Sr and Zn ions may respectively act as a network modifier and network former when they are

Table 2
The relative ratio between IR absorbance for Si–O groups with BO and NBO atoms as well as Tg of different glasses.

Bands ratio	BG-Ca	BG-Sr	BG-Zn
Si–O–Si (asym)/Si–O–NBO	1.26 ± 0.02	1.23 ± 0.01	1.31± 0.03
Si–O–Si (sym)/Si–O–NBO	0.25 ± 0.03	0.26 ± 0.04	0.32 ± 0.03
Tg (°C)	760	750	716

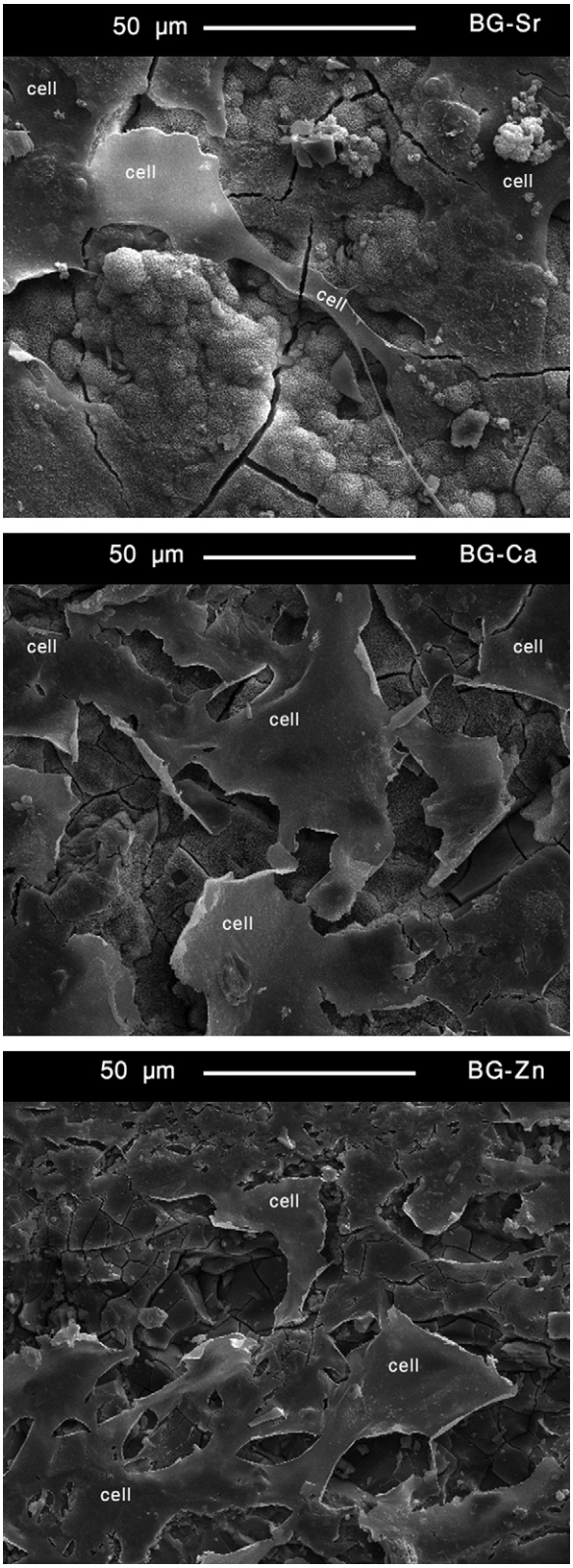

Fig. 10. Morphology of the osteolastic cells cultured on different glass samples after 14 days of incubation.

replaced for Ca. Also, the changes in glass transition temperatures indicate that the addition of ZnO results in a weakened network. It is suggested that like Mg [16], zinc ions can also form tetrahedral ZnO_4^{2-} species which require Ca ions

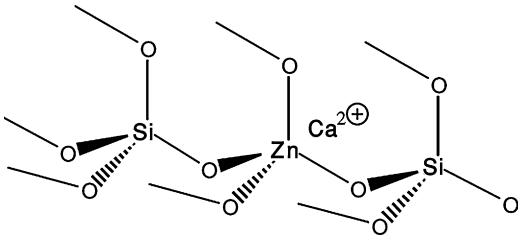

Fig. 11. Cartoon of the BG-Zn glass structure. This illustrates the zinc cations within the silicate network as tetrahedral ZnO_4 units charge balanced by calcium ions.

for charge balancing. This removes cations from the silica network and increase numbers of bridging oxygen. The newly formed Si–O–Zn bonds (Fig. 11) have significantly lower bond strength than Si–O–Si bonds in the silicate chain, which leads to decrease in Tg. For the Sr substitution however, it seems that Sr ion is exchanged with Ca ions in the same position and no considerable change in Tg and number of BO occurs. The minor decrease in Tg observed for BG-Sr can be due to the lower bond strength of –O–Sr compared to –O–Ca (because of the same electrical charge and the higher ionic radius of Sr compared to Ca).

Different in vitro bioactivity behavior of the glasses can be described by the different role of each substituted ions within the network. It was found that Zn ions may reduce number of non-bridging oxygen atoms and hence decrease glass bioactivity through reduction of glass dissolution. Furthermore, Sr ions did not change concentration of bridging oxygen atoms; but a network expansion may occur due to the substitution of Ca ions by the larger Sr ions which results in faster glass degradation. However, there are some important points which should be taken in to account:

The rate of glass degradation (network disruption) can be approximated by measuring the change in Si concentration of SBF during soaking so that the higher amount of Si, the greater degradation of glass specimen [11]. Regarding to the above mentioned comments, the release of Si ions from the BG-Sr glass should be higher than that of other samples, while the concentration of Si ions at the early stage of soaking is nearly the same for all specimens and then a sharp decrease is observed for BG-Sr and BG- Ca. After 24 h, the least level of Si ions in the SBF solution belongs to BG-Sr specimen (Fig. 2). Based on the bioactivity mechanism, the Si–O–Si bands in the glass structure break into Si–OH groups as a result of ion exchanging process between the glass surface and the solution:

$$\mathrm{Si{-}O{-}Si + H{-}OH = Si{-}OH + Si{-}OH} \quad (1)$$

This leads to release of Si as Si–OH ions into the SBF as well as formation of Si–OH groups in the glass-solution interface. Then a silica (Si–O–Si) rich layer is formed on the glass surface through condensation of Si–OH groups existed in the glass surface and SBF solution [18].

$$\mathrm{Si{-}OH + Si{-}OH = Si{-}O{-}Si + H_2O} \quad (2)$$

It seems that this condensed layer is formed on the surface of all samples because the intensity of Si–O–Si bands in FTIR

spectra sharply improved after immersing in SBF solution (Fig. 3). Increasing in band intensity of H_2O at about 3450 cm^{-1} in FTIR spectra of soaked sample can be due to the water molecules trapped in the silica-rich layer. Loss in Si concentration of the SBF is probably due to the inhibitory effect of calcium phosphate layer formed on glass surfaces during soaking and contribution of Si ions in the lattice of calcium phosphate layer to form silicate-containing phase. For BG-Zn, there is no restriction for Si release and thus a nearly continues profile is achieved.

The presence of P element in EDS patterns (Fig. 8) reveals that calcium phosphate layer precipitates on BG-Zn. Comparing the EDS patterns of the soaked samples suggests the presence of a thin calcium phosphate layer for BG-Zn, because of the same diffusion depth of irradiated electron beam and the higher peak intensity of Si element in EDS pattern of the BG-Zn compared to other samples. It denotes that the compositional information is entered from the inferior phase (glass) which shows the thin thickness of the precipitated layer.

Based on the XRD and EDS data, it can be stated that the calcium phosphate layer formed on BG-Zn is amorphous in nature. Furthermore, the crystallinity of the calcium phosphate layer formed on BG-Sr is higher than BG-Ca. It is proposed that the use of a bioactive glass comprising a source of Sr results in replacing a proportion of the Sr^{2+} ions into the apatite phase, providing a mixed Sr^{2+}/Ca^{2+} carbonated apatite. This Sr^{2+} substituted apatite has a lower solubility than unsubstituted apatite [19], leading to an increase in the rate of apatite deposition.

5. Conclusions

Incorporation of 5 mol.% of strontium and zinc ions in the sol–gel derived SiO_2–CaO bioglass alters temperatures of structural phenomena such as glass transition and crystallization. Zinc was found that increases the average of bridging oxygen atoms on the glass structure but diminishes network stability. It is found that strontium ions in the glass composition provoke apatite formation whereas zinc ions inhibit the precipitation and growth of calcium phosphate phase. Both strontium and zinc ions exhibit stimulating effect on osteoblastic cells by increasing alkaline phosphatase activity and rate of proliferation, respectively. Although both SBF and in vitro cell culture tests are useful as initial experiments, promising materials should be followed up with in vivo animal studies.

References

[1] W. Vogel, W. Holand, Development, structure, properties and application of glass–ceramics for medicine, J. Non-Cryst. Solids 123 (1990) 349–353.
[2] L.L. Hench, Bioceramics: from concept to clinics, J. Am. Ceram. Soc. 74 (1991) 1487–1510.
[3] J. Ma, C.Z. Chen, D.G. Wang, X.G. Meng, J.Z. Shi, Influence of the sintering temperature on the structural feature and bioactivity of sol–gel derived SiO_2–CaO–P_2O_5 bioglass, Ceram. Int. 36 (2010) 1911–1916.
[4] J. Buehler, P. Chappuis, J.L. Saffar, Y. Tsouderos, A. Vignery, Strontium ranelate inhibits bone resorption while maintaining bone formation in alveolar bone in monkeys, Bone 29 (2001) 176–179.
[5] A. Oki, B. Parveen, S. Hossain, S. Adeniji, H. Donahue, Preparation and in vitro bioactivity of zinc containing sol–gel-derived bioglass materials, J. Biomed. Mater. Res. A 69 (2004) 216–221.
[6] V. Aina, G. Malavasi, A. Fiorio Pla, L. Munaron, C. Morterra, Zinc-containing bioactive glasses: surface reactivity and behaviour towards endothelial cells, Acta Biomater. 5 (2009) 1211–1222.
[7] S. Hesaraki, M. Gholami, S. Vazehrad, S. Shahrabi, The effect of Sr concentration on bioactivity and biocompatibility of sol–gel derived glasses based on CaO–SrO–SiO_2.P_2O_5 quaternary system, Mater. Sci. Eng. C 30 (2010) 383–390.
[8] J. Lao, E. Jallot, J.M. Nedelec, Strontium-delivering glasses with enhanced bioactivity: a new biomaterial for antiosteoporotic applications, Chem. Mater. 20 (2008) 4969–4973.
[9] T. Kokubo, H. Kushitani, S. Sakka, T. Kitsugi, T.J. Yamamuro, Solutions able to reproduce in vivo surface-structure changes in bioactive glass-ceramic A-W, J. Biomed. Mater. Res. 24 (1990) 721–734.
[10] S. Hesaraki, M. Alizadeh, H. Nazarian, D. Sharifi, Physico-chemical and in vitro biological evaluation of strontium/calcium silicophosphate glass, J. Mater. Sci. Mater. Med. 21 (2010) 695–705.
[11] P. Saravanapavan, J.R. Jones, S. Verrier, R. Beilby, V.J. Shirtliff, L.L. Hench, Binary CaO–SiO_2 gel-glasses for biomedical applications, Biomed. Mater. Eng. 14 (2004) 467–486.
[12] Y. Kim, A.E. Clark, L.L. Hench, Early stages of calcium–phosphate formation in bioglasses, J. Non-Cryst. Solids 113 (1989) 195–202.
[13] M.D. O'Donnell, R.G. Hill, Influence of strontium and the importance of glass chemistry and structure when designing bioactive glasses for bone regeneration, Acta Biomater. 6 (2010) 2382–2385.
[14] Y. Gotoh, K. Hiraiwa, M Nagayama, In vitro mineralization of osteoblastic cells derived from human bone, Bone Miner. 8 (1990) 239–250.
[15] J. Ma, C.Z. Chen, D.G. Wang, J.Z. Shi, Textural and structural studies of sol–gel derived SiO_2–CaO–P_2O_5–MgO glasses by substitution of MgO for CaO, Mater. Sci. Eng. C 30 (2010) 886–890.
[16] S.J. Watts, R.G. Hill, M.D. O'Donnell, R.V. Law, Influence of magnesia on the structure and properties of bioactive glasses, J. Non-Cryst. Solids 356 (2010) 517–524.
[17] L. Linati, G. Lusvardi, G. Malavasi, L. Menabue, M.C. Menziani, P. Mustarelli, U. Segre, Qualitative and quantitative structure-property relationships (QSPR) analysis of multicomponent potential bioglasses, J. Phys. Chem. B 109 (2005) 4989–4998.
[18] R. Hill, An alternative view of the degradation of bioglass, J. Mater. Sci. Lett. 15 (1996) 1122–1125.
[19] R. Hill, Bioactive glass, Patent Cooperation Treaty, WO 2007/144662.